

# Charge sign dependence of cosmic ray modulation near a rigidity of 1 GV

J. M. Clem, P. Evenson,<sup>1</sup> D. Huber,<sup>2</sup> and R. Pyle

Bartol Research Institute, University of Delaware, Newark

C. Lopate and J. A. Simpson

Laboratory for Astrophysics and Space Research, University of Chicago, Chicago, Illinois

**Abstract.** New observations of electron fluxes made in 1997 and 1998 extend our ongoing investigation of the relative modulation of positively and negatively charged particles. We compare electron fluxes measured on high-altitude balloon flights with continuing observations of helium fluxes from the IMP 8 spacecraft and present new measurements of the primary cosmic ray positron abundance in 1997 and 1998. Electron fluxes during the 1984–1990 period show a flat topped distribution, whereas the positively charged He fluxes show a peaked distribution, with the peak in 1987. This is expected from modulation theory, including the role of drifts when the northern heliospheric magnetic field is inward, and the southern heliospheric field is outward. From 1990 to 1999, data are consistent with an inverse relationship, but electron data are too sparse to allow a definitive statement. Near a rigidity of 1 GV the relative abundance of electrons and helium nuclei is a weak function of the tilt angle of the heliospheric current sheet.

## 1. Introduction

Although the Sun has a complex magnetic field, the dipole term nearly always dominates the magnetic field of the solar wind. The projection of this dipole on the solar rotation axis ( $A$ ) can be either positive, which we refer to as the  $A^+$  state, or negative, which we refer to as the  $A^-$  state. Near each sunspot maximum the dipole reverses direction, leading to alternating magnetic polarity in successive solar cycles. *Babcock* [1959] was the first to observe a change in the polarity state when he observed the northern (southern) polar region change to positive (negative) polarity, that is, a transition to the  $A^+$  state. Many modulation phenomena have different patterns in solar cycles of opposite polarity. Possibly, the most striking of these is the change in the flux of electrons relative to that of protons and helium when the solar polarity reverses [Evenson and Meyer, 1984; Garcia-Munoz *et al.*, 1986; Ferrando *et al.*, 1996].

Electromagnetic theory has an absolute symmetry under simultaneous interchange of charge sign and magnetic field direction, but positive and negative particles can exhibit systematic differences in behavior when propagating through a magnetic field that is not symmetric under reflection. Two systematic deviations from reflection symmetry of the interplanetary magnetic field have been identified (one in the large-scale field, the other in the turbulent, or wave component). The Parker field has opposite magnetic polarity above and below the helioequator, but the spiral field lines themselves are mirror images of each other. This antisymmetry produces drift velocity fields that (for positive particles) converge on the

heliospheric equator in the  $A^+$  state or diverge from it in the  $A^-$  state [Jokipii and Levy, 1977; Jokipii, 1997]. Negatively charged particles behave in the opposite manner, and the drift patterns interchange when the solar polarity reverses. Alternatively, systematic ordering of turbulent helicity discovered by *Bieber et al.* [1987] can cause diffusion coefficients to depend directly on charge sign and polarity state.

Accurate measurements of the relative modulation of negative and positive electrons (negatrons and positrons) are beginning to enable a more precise investigation of the “pure” charge sign dependence of modulation. One major finding of these studies is that the positron abundance is at most 20% in data taken during the  $A^+$  polarity decade of the 1990s. Since this polarity state is the one expected to enhance the positron fluxes, this reduces the impact of concerns such as that voiced by *Moraal et al.* [1991] that the positron content of the electrons might be so high as to challenge their use as negative particles in charge sign studies. Historical data on the differential modulation of electrons and nuclei can now be approached with new confidence as a way to study the lack of reflection symmetry in solar wind magnetic fields.

## 2. Observations

In this paper we report new measurements of the 1.2-GV electron flux (both negatron and positron) taken in 1997 and 1998, by the balloon-borne payload LEE/AESOP [Hovestadt *et al.*, 1970; Clem *et al.*, 1996]. In the appendix we discuss improvements in the AESOP instrument and data analysis process over that presented by *Clem et al.* [1996]. We also present an extension of measurements made by the University of Chicago instrument on IMP 8 of helium in the energy range 160 to 220 MeV/nucleon. These new data are shown in Figure 1, along with previous data, as a function of time. LEE data have been reduced in the standard way [Evenson *et al.*, 1995; Fulks, 1975]. The IMP 8 analysis is primarily unchanged, but the data are presented with higher time resolution and therefore larger

<sup>1</sup>Also at National Science Foundation, Arlington, Virginia.

<sup>2</sup>Now at Research Support Instruments, Lanham, Maryland.

Copyright 2000 by the American Geophysical Union.

Paper number 2000JA000097.  
0148-0227/00/2000JA000097\$09.00

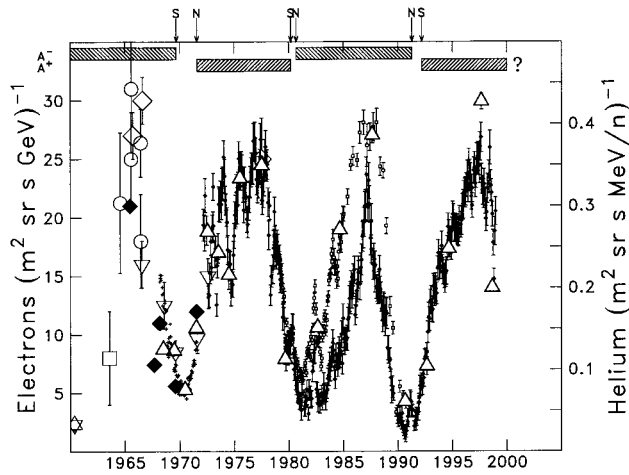


**Figure 1.** Time profile of particle measurements with rigidities of roughly 1.2 GV. Open symbols represent electron data, and solid symbols represent helium data. Also shown is the solar magnetic polarity state and the symbols N and S signify the time these polar regions change polarity state. *Evenson* [1998] gives references to the historical electron data.

statistical errors than in the past. Solar polarity reversals, derived from magnetogram observations taken over the last four solar cycles [*Babcock*, 1959; *Howard*, 1974; *Webb et al.*, 1984; *Lin et al.*, 1994], are also documented in Figure 1. The symbols “N” and “S” show the best estimates of when the polar regions reversed polarity. The polarity reversals are based on data from heliographic latitudes  $>70^\circ$ , except for the first, which covers  $50^\circ$ – $80^\circ$  latitude in each hemisphere. The plotting scales for electrons and helium were originally chosen to normalize the fluxes in the 1970s, and we have used these scales consistently in our reports ever since. In this representation the fluxes of the two species are consistently different during the 1980s, but again virtually coincide in the 1990s. The exceptions, which occur at solar minimum in both decades, are discussed in some detail below.

To place the new LEE data into context with other electron data, Figure 2 shows (with an arbitrary normalization) the counting rate of 2.5-GeV electrons measured by *Ulysses* [*Heber et al.*, 1999a, b]. Our series of measurements of the electron flux at 2.2 GeV is shown as solid triangles, while the 1.2-GeV measurements shown in Figure 1 are repeated as open triangles. Two important conclusions follow from Figure 2. One is that there is good consistency between the LEE data and the *Ulysses* KET data at nearly the same energy. The second is that the modulation of electrons is highly energy dependent. Preliminary KET data for electrons at lower energy are consistent with the LEE data, but the investigators are not at present prepared to publish these data (*B. Heber*, private communication, 1999). As we show later, the time structure of the electron fluxes at the time of the LEE flight in 1997 is particularly interesting, and we are working with the KET team to produce a comprehensive picture of the evolution of electron fluxes in time and energy during this period.

In addition to the obvious dependence of modulation on energy, other factors make straightforward interpretation of our observations difficult. In Table 1 we summarize the kinematic properties of particles relevant to this discussion. One issue is the spectral shape, as pointed out by *Bieber et al.* [1999]. Figure 2 presents electron fluxes at 1.2 and 2.2 GeV with the

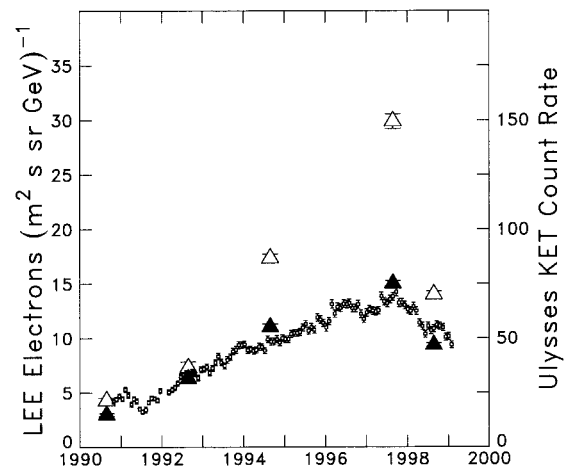


**Figure 2.** Comparison of electron observations from 1990 to 1999. Small, open circles give the counting rate of 2.5-GeV electrons measured by the *Ulysses* spacecraft, with arbitrary normalization. Solid triangles show the flux of electrons measured at 2.2 GeV by the LEE payload. Open triangles present the flux of 1.2-GeV electrons from LEE, also shown in Figure 1.

same normalization, showing that the electron spectrum in this energy range is nearly flat near solar maximum, but has a significant, negative slope at solar minimum. On the other hand, the helium spectrum has a positive slope at all times from 160 to 220 MeV/nucleon. There is also a major velocity difference between electrons and helium. Recently, interest in velocity as a parameter in its own right has increased with the development of dynamic models of particle scattering in the interplanetary magnetic field [*Bieber et al.*, 1994].

There is not even agreement on the parameterization to give the best phenomenological description of modulation. Historically, *McDonald* and coworkers have considered the product of velocity and rigidity to be the most useful parameter [*Fujii and McDonald*, 1995; *McDonald*, 1998], while we have focused on rigidity alone. Which approach one adopts has major observational consequences. As Table 1 shows, picking rigidity or beta times rigidity correspond roughly to selecting either the open or closed triangles in Figure 2. In other words, this choice can lead to qualitatively different behavior of the particles selected for comparison.

Since positrons and negatrons of the same rigidity have the same velocity, systematic observations of positrons will eliminate this source of uncertainty in the attempt to isolate a component of modulation that is fundamentally charge-sign-dependent. Figure 3 shows a selective compilation of published data on the positron abundance in the energy range most relevant to the modulation problem. In this paper, we use the term “abundance” consistently to mean the ratio of one component of a population to the total population. Thus the positron abundance is (positron flux)/(positron flux + negatron flux). *Evenson* [1998] and *Clem et al.* [1996] discuss the selection of data taken prior to 1994; all data published since then are included in Figure 3. We also include in Figure 3 the new measurements of the positron abundance made by Anti-Electron Suborbital Payload (AESOP), plotting the weighted average of measurements made in 1997 and 1998, since the individual measurements are statistically indistinguishable.

**Table 1.** Kinematic Properties of Particles Discussed in This Study

Particle	Energy	$\gamma$ Lorentz Factor	$\beta(v/c)$	Rigidity, GV	$\beta \times$ Rigidity, GV
Electron	1.2 GeV	2350	0.9996	1.2	1.2
Electron	2.2 GeV	4306	0.9998	2.2	2.2
Electron	2.5 GeV	4893	0.9998	2.5	2.5
Helium	160 MeV/nucleon	1.172	0.5211	1.14	0.59
Helium	220 MeV/nucleon	1.236	0.5878	1.35	0.80

### 3. Discussion

Both drifts and helicity can operate at the same time, and observations as to which may dominate are ambiguous, partly because specific predictions are highly model dependent. Models including particle drifts are quite sensitive to the geometry of the heliospheric current sheet, leading to a natural prediction of the apparent alternation of “flat” and “peaked” solar cycles. An inescapable prediction is that a flat cycle in positive particles should be peaked in negative, and vice versa. Examining Figure 1, the electron profile in the 1980s is much flatter than that of the helium, but much of the difference in the apparent shape comes from the abrupt rise and fall of the helium flux during 1987. Below we explore at some length the possibility that this may be a somewhat different phenomenon from that which produces the alternating flat and peaked cycles at higher energy.

Our new data suggest that the inverse phenomenon may have occurred in 1997. Although a time dependence can hardly be extracted from the three electron points in 1994, 1997, and 1998, the return to the same relative normalization of electrons and helium chosen for the 1970s is quite dramatic, except for the point in 1997. Clearly, further analysis of Ulysses data to extend the validated data to lower energy is of great importance in investigating this sudden excursion in the flux of one species but not the other. We also note that no such feature was observed in the 1970s, although it could have occurred

between LEE flights and thus not been detected. The remarkable tracking of electron and helium fluxes during the 1970s was what led *Bieber et al.* [1987] to postulate magnetic helicity as potential source of charge sign dependence.

*Smith* [1990] investigated the relationship between cosmic ray fluxes and the “tilt angle” of the heliospheric current sheet. Using data from the Deep River neutron monitor, with an median response rigidity of  $\sim 16$  GV [*Ahluwalia and Wilson*, 1997], he showed that the regression relationship was different during epochs of opposite magnetic polarity. *Heber et al.* [1999a, b] have recently reported that the variation in the relative flux of protons and electrons at 2.5 GV (at the Ulysses spacecraft) is also ordered by this tilt angle. For times since 1976, estimates of the tilt angle of the solar dipole are available on the web page <http://quake.stanford.edu/~wso/Tilts.html>. Using the mean position of the maximum extent of the current sheet (“new method”) as a measure of tilt angle, Figure 4 shows the electron (from balloon flights) to helium (from IMP 8) flux ratio at 1.2 GV as a function of tilt angle. Solid symbols indicate  $A^-$  measurements and open symbols denote  $A^+$ . The lowest  $A^-$  flux ratio is, indeed, from 1987, and the highest  $A^+$  flux ratio is from 1997. However, neither of them corresponds to the lowest observed tilt angle. A closer look at the phenomenon in 1987 (when all data are available with good time resolution) is shown in Figure 5, where it is clear that the “spike” in the helium flux does not correspond directly to a feature in the tilt angle. The end of the enhanced helium flux clearly coincides with the rise of the tilt angle in the new solar

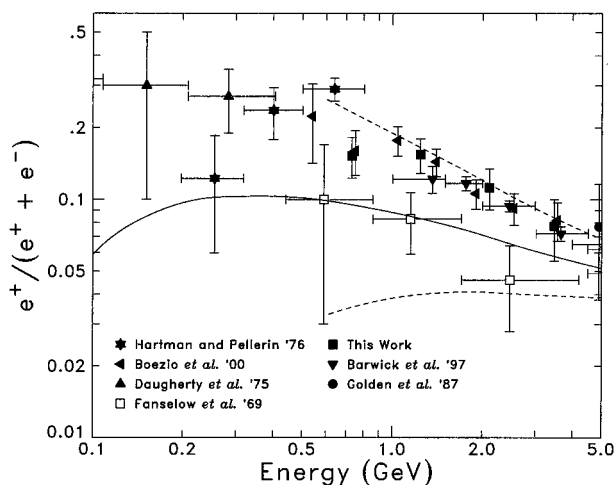


**Figure 3.** Compiled measurements and calculations of the positron fraction as a function of energy for different epochs of solar magnetic polarity. Solid line is the modulated positron fraction calculated by *Protheroe* [1982]. Dashed lines are from *Clem et al.* [1996] for  $A^+$  (top line) and  $A^-$ . Solid symbols show data taken in the  $A^+$  state, while the open symbols give the only observation taken in the  $A^-$  state.

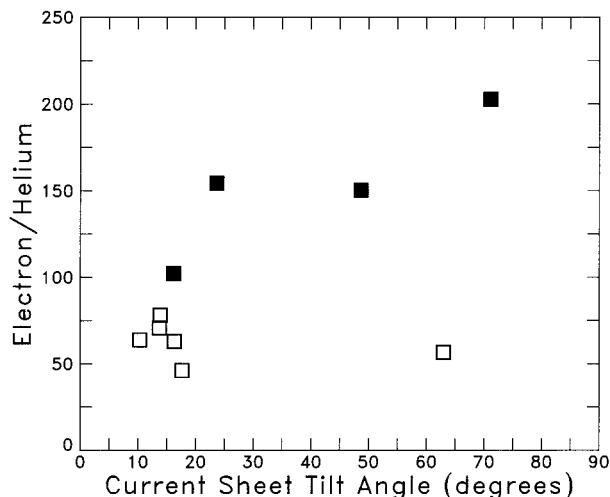


**Figure 4.** The ratio of the electron (balloon flights) to helium flux (IMP 8) at 1.2 GV as a function of the maximum extension of the heliospheric current sheet or “tilt angle.” Solid symbols indicate  $A^-$ , and open symbols represent  $A^+$  polarity state.

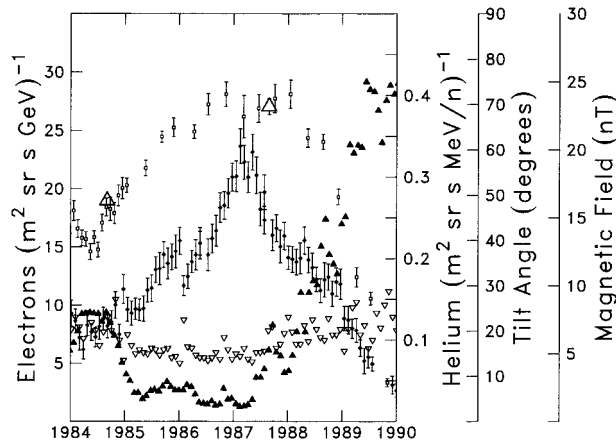


**Figure 5.** Expansion of Figure 1 with the addition of 27-day averages of the heliospheric magnetic field tilt angle (solid triangles) and vector magnitude (open inverted triangles).

cycle, but the tilt angle was low throughout most of 1986, when the helium flux simply follows the gradual rise in the electron flux. If anything, the start of the helium spike may coincide with the brief rise in the tilt angle in late 1986.

Recently, *Cane et al.* [1999] have noted the importance of the amplitude of the average interplanetary magnetic field as an organizing parameter for the level of solar modulation. When seen in the context of recent work relating solar irradiance to solar magnetic activity [*Lockwood and Stamper*, 1999] this simple, yet general concept also provides a consistent explanation for the excellent correlation between historical records of cosmic ray modulation (cosmogenic isotopes) and historical proxies for solar irradiance variations [*Lean et al.*, 1995]. We therefore examined the possibility of a relation between the helium spike and the field amplitude (vector magnitude from the NSSDC OMNI data set) also shown in Figure 5. Again, the results are inconclusive. There is more scatter in the field amplitude than in the tilt angle, but apart from this, the two quantities track each other very closely.

In 1987 the helium spike is not accompanied by a corresponding electron ravine. The brevity of the spike and the lack of explicit relationship to tilt angle may mean that it requires some modification of the simplest interpretation of the alternating flat and peaked solar cycles [*Jokipii and Levy*, 1977]. The spike can possibly be understood in general terms by observing that the particles that drift away from the current sheet have much larger radial gradients than those that drift toward it. The intensity of particles having large gradients is more sensitive to any change in the heliosphere than that of particles with small gradients.

At higher rigidities and/or at times when the tilt of the current sheet is large, the leading term of the response may be to the tilt angle. However, the low rigidity helium spike may result from some other, more subtle modification of the interplanetary field configuration associated directly with the emergence of the first flux of the new cycle. For example, *Fisk* [1996] argues that photospheric magnetic fields may have direct connections with heliospheric fields, even at quite high latitude. In any event the appearance of the helium spike does not coincide with an excursion in any of the commonly used parameters describing the interplanetary magnetic field.

Our failure to find a correlation between flux ratio and tilt

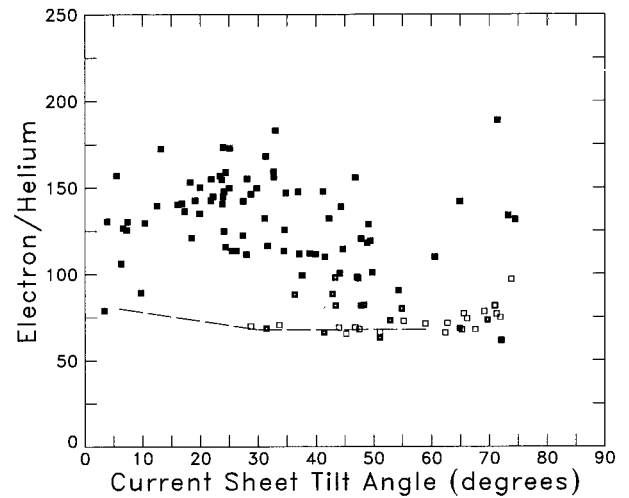


**Figure 6.** Higher time resolution version of Figure 4 using electron measurements taken between 1978 and 1992 from ISEE 3/ICE. Solid symbols indicate the  $A^-$  polarity state, open symbols the  $A^+$  polarity state, and half-open symbols indicate an undefined configuration. The dashed line is the observation of *Heber et al.* [1999] comparing electrons to protons at higher rigidity.

angle does not contradict *Heber et al.* [1999a, b], who observe approximately a 15% rise in the electron to proton flux ratio with decreasing tilt angle in the  $A^+$  polarity state. Their observation was made with 2.5 GV electrons, whereas our observation is at 1.2 GV and as noted earlier, there are major differences in the modulation of electrons at these two energies. Furthermore, the magnitude of the effect seen at Ulysses is small compared to the fluctuations in our data. We illustrate this in Figure 6, showing the ratio of electron fluxes at 1.2 GeV from the University of Chicago electron experiment on the ISEE 3/ICE mission to helium fluxes at 160–220 MeV/nucleon from IMP 8. Data from the  $A^-$  state show a slight tendency to lower values at low tilt angle, but the scatter is large. Otherwise, there is little evidence of a significant trend. The variation in the electron to proton ratio during the  $A^+$  state reported by *Heber et al.* [1999a, b] is shown by the dashed line, with an arbitrary normalization. Given the scatter of the data, such a dependence may or may not be present. The overwhelming impression from Figure 6 is the major shift in the relative abundance of electrons and helium related to the polarity reversal.

Finally, we address the implications of measurements of positron abundance. In Figure 3 the solid line shows the calculation of *Protheroe* [1982] of the positron abundance including modulation, but not charge sign dependence. The dashed lines give the prediction of *Clem et al.* [1996] for the positron abundance in opposite solar polarity states using the observed variation in electron fluxes relative to nuclei in the opposite polarity states. This prediction, made before any of the data shown from the 1990s were taken, proved to be quite accurate for the  $A^+$  epoch, and is basically consistent with the pioneering data from the  $A^-$  epoch. However it's also possible [*Moskalenko and Strong*, 1998] to interpret the observations in terms of production of secondary positrons in the interstellar medium.

Figure 7 shows measurements of the positron abundance at  $\sim 1.3$  GV as a function of time, along with the prediction of

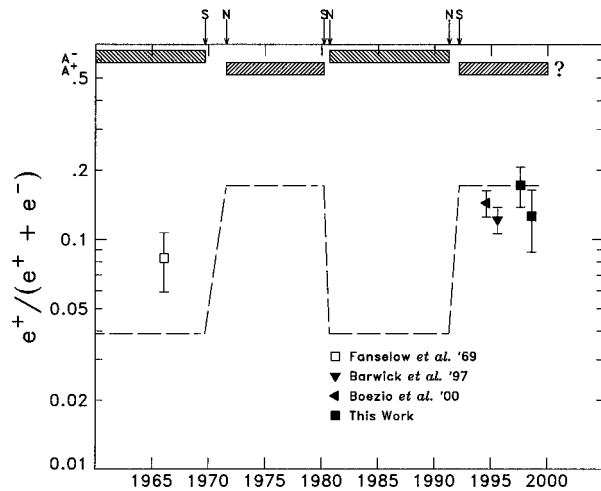


**Figure 7.** Time profile of the positron abundance at  $\sim 1.3$  GeV.

*Clem et al.* [1996]. During the 1990s, four measurements have been made that agree with each other within errors and are consistent with the *Clem et al.* [1996] prediction. The only other observation near this energy was taken during the 1960s. Taken in isolation, it is marginally consistent with the abundances measured in the 1990s. Referring back to Figure 3, however, it is difficult to believe that the overall positron abundance observed in the 1960s was not significantly lower than in the 1990s. However, the question of whether the specific *Clem et al.* [1996] prediction for  $A^-$  is correct or not is still quite open to further measurement.

Although our data for 1997 and 1998 are statistically indistinguishable and are combined for Figure 3, we present the points individually in Figure 7 because the measurements were taken at two interesting times. The 1997 measurement corresponds to a possible electron spike, the inverse of the 1987 phenomenon in helium discussed in detail above, yet if anything the positron abundance is higher than normal at that time. However, statistical significance is marginal.

The 1998 measurement was taken during a significant Forbush decrease, during which the helium and electron fluxes seem to move together (Figure 1) and there is little change in the positron abundance. If a constant positron abundance could be confirmed with better statistics, and better time resolution, it would indicate that particle drifts play no significant role in producing a Forbush decrease.

#### 4. Conclusions

In this paper, we have focused on charge sign dependent solar modulation at rigidities around 1 GV by considering changes in the relative flux level of electrons and helium nuclei. Our new data confirm the well-established result that there are major shifts in the relative abundance of these two species when the solar magnetic polarity changes, but only minor variations during the intervening years. The major shifts appear to be a phenomenon of the outer heliosphere (that is beyond 5 AU) because the amplitudes are factors of 2 or 3, while radial and latitudinal gradients of both electrons and nuclei in the inner heliosphere are at most a few percent.

At 1.2 GV the variations in the electron to helium flux ratio exhibit little ordering by the current sheet tilt angle. We have

also tentatively identified a new phenomenon in the 1.2-GV data in which a brief spike in the flux of the more heavily modulated charge sign immediately precedes the onset of the new modulation cycle. This is clearly observed in the high time resolution electron and helium data in 1987, and consistent with the data in 1997, where the sparsity of electron data preclude a definitive statement.

A consistent baseline, with agreement of several separate measurements, has been established for the positron abundance during the  $A^+$  epoch of the 1990s. Continued, periodic, measurements of positron abundance through the current solar polarity reversal should provide a definitive control for the role of particle velocity in the modulation process, and isolate a pure charge sign effect. Unfortunately, the availability of high time resolution, high statistical accuracy positron abundance measurements required to understand the spike phenomenon is uncertain at best over the coming solar minimum.

#### Appendix

Anti-Electron Suborbital Payload (AESOP) resolves positrons and negatrons with a maximum detectable rigidity of 6 GV [*Clem et al.*, 1996]. AESOP and LEE [*Hovestadt et al.*, 1970] were launched together as a single balloon payload on September 1, 1997, and August 29, 1998, from Lynn Lake, Manitoba, achieving a flight duration of roughly 20 and 36 hours, respectively. Both flights were successful and provided clean data for analysis. AESOP has been enhanced with a gas Cherenkov detector, and the data analysis has been improved since the work of *Clem et al.* [1996]. In this appendix we outline our current procedure.

Primary electrons with rigidities below the local geomagnetic cutoff are not present inside the atmosphere; however, primary nucleons above the cutoff enter the atmosphere and produce secondary electrons with rigidities above and below the cutoff. These interactions produce knock-on electrons and short-lived particles such as pions and kaons which decay (via muons) into positrons and electrons. The total electron flux as a function of depth reaches a broad maximum at  $100 \text{ g/cm}^2$ , while the abundance of primary electrons in the total electron population decreases with increasing depth.

Upward moving secondary electrons that lack sufficient rigidity to escape the magnetosphere spiral along the geomagnetic field lines and reenter the atmosphere at conjugate points on the opposite side of the magnetic equator [*Barwick et al.*, 1998]. These are known as reentrant albedo particles, and at high magnetic latitude they are a time dependent phenomenon. Diurnal intensity variations of electron intensities with low rigidities were first correctly interpreted by *Jokipii et al.* [1967], who explained this effect as an interaction of the solar wind with the magnetosphere. At some locations, such as Lynn Lake, Manitoba, field lines connect conjugate magnetic locations during the day but are drawn out into the geotail during the night, causing both the cutoff and reentrant albedo particles to disappear at night and reappear during the day.

To determine the primary abundance, observations must be taken at energies above the (time varying) geomagnetic cutoff, the secondary component must be appropriately removed. We do this from calculations of the positron abundance in secondaries, together with information on the cutoff and the secondary electron flux determined by the standard analysis methods for the larger-acceptance LEE instrument [*Fulks and Meyer*,

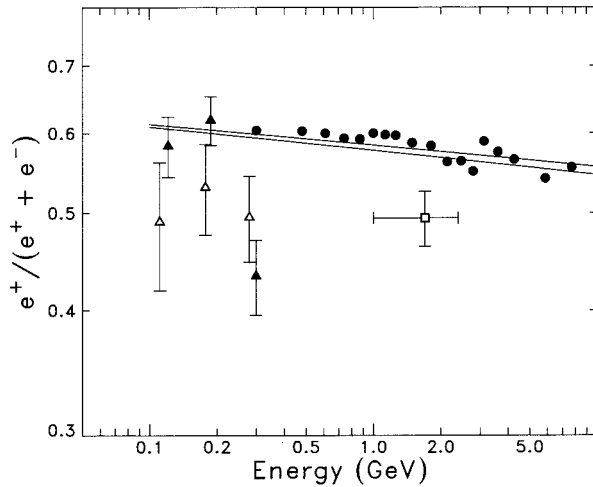


**Figure A1.** Positron abundance in atmospheric secondary and reentrant albedo particles. Calculations: Solid circles, *Boezio et al.* [2000] for  $3.9 \text{ g/cm}^2$ ; top line, this work at  $2.7 \text{ g/cm}^2$ ; bottom line, this work at  $4.0 \text{ g/cm}^2$ . Observations: open square, *Barwick et al.* [1998]; open triangles, this work, day data; solid triangles, this work, night data. Some points have been offset slightly to improve visibility of the error bars.

1974; *Fulks*, 1975]. After a bit of algebra the primary positron abundance can be determined from the following relationship:

$$P_P^A = \frac{P_M^A - S_M^L P_C^S}{1 - S_M^L}, \quad (\text{A1})$$

where  $P_P^A$  represents primary positron abundance,  $P_M^A$  is the positron abundance as measured by AESOP,  $P_C^S$  is the calculated positron abundance in secondary electrons, and  $S_M^L$  is the secondary abundance as measured by LEE. This convenient relationship allows a simple transformation of the observed positron abundance to the primary positron abundance at the observation depth (roughly  $2.7 \text{ g/cm}^2$  for both flights). Attenuation of primary electrons at this depth is significant but is nearly identical for positrons and negatrons, so this cancels out and is not considered. Primary abundances determined from (A1) are used in the figures and discussion in the paper.

In addition to the primary positron abundance, we can also extract information about the secondary electrons from our data. Figure A1 displays the results of two separate calculations of atmospheric secondary abundances. We have done a Monte-Carlo calculation using FLUKA [*Fassò et al.*, 1993, 1997] shown by the solid lines. The bottom line and solid circles [*Boezio et al.*, 1999] were both calculated at a depth of  $4.0 \text{ g/cm}^2$  while the top line was determined for  $2.7 \text{ g/cm}^2$ . The two calculations agree well if we assume the structures in the *Boezio et al.* [2000] calculation are random statistical fluctuations. For the work in this paper we have used our own calculation.

We also show some observations in Figure A1, taken in the intermediate zone (Lynn Lake, Manitoba) and separated into (geomagnetic) “night” and “day” using the time structure of the total electron fluxes at lower energy from LEE. Unfortunately, the geomagnetic field was rather unsettled during both flights, so the analysis is not as complete as one might hope. The daytime measurements were taken during the 1997 flight, while the nighttime measurements were taken only during the

1998 flight. Only observations below the maximum daytime vertical cutoff ( $\approx 300 \text{ MV}$ ) are shown in this figure.

Daytime data are dominated by reentrant albedo. Also shown is the *Barwick et al.* [1998] measurement taken in the equatorial region (Fort Sumner, Texas) where the effective vertical geomagnetic cutoff is roughly constant at  $\sim 4.5 \text{ GV}$ . These measurements indicate that the positron abundance in the reentrant albedo has very little energy dependence between 0.1 and 2.4 GeV.

Reentrant albedo particles are not present in geomagnetic-night observations that consist only of secondary and primary electrons. The three points shown are for energies at which the analysis from LEE indicated that the flux consisted primarily (over 99%) of secondary particles. For the two lowest points the observed positron abundance is fully consistent with the calculation. The abundance at 279 MeV clearly indicates that we are observing a significant flux of primary particles (dominated by negatrons) in contradiction of the analysis from LEE. We do not consider this a serious problem, primarily because we treat rather large energy intervals as if they were concentrated at the center point. The adjacent energy interval (446 MeV) was reported as having 67% secondaries (at  $2.75 \text{ g/cm}^2$ ). Note that (Figure 3) we only begin to have real confidence in our primary positron abundance determination at the point plotted at 731 MeV.

**Acknowledgments.** We would like to thank Andrew McDermott, Leonard Shulman, James Roth, and Gerald Poirier for their technical assistance with the balloon payloads. We also want to thank the crew of the National Scientific Balloon Facility. This work was partially supported by NASA under grant NAG 5-2606 and by NSF under grant ATM-9632323.

Janet G. Luhmann thanks Garry M. Webb and Harm Moraal for their assistance in evaluating this paper.

## References

- Ahluwalia, H., and M. Wilson, Cycle 22 recovery for cosmic ray modulation, *Proc. 25th Int. Cosmic Ray Conf. Durban*, 2, 53, 1997.
- Babcock, H. D., The Sun’s polar magnetic field, *Astrophys. J.*, 130, 364–365, 1959.
- Barwick, S. W., et al., Measurements of the cosmic-ray positron fraction from 1 to 50 GeV, *Astrophys. J.*, 482, L191–L194, 1997.
- Barwick, S. W., et al., Cosmic ray reentrant electron albedo: High Energy Antimatter Telescope balloon measurements from Fort Sumner, New Mexico, *J. Geophys. Res.*, 103, 4817–4823, 1998.
- Bieber, J., P. Evenson, and W. H. Matthaeus, Magnetic helicity of the IMF and the solar modulation of cosmic rays, *Geophys. Res. Lett.*, 14, 864–867, 1987.
- Bieber, J., W. H. Matthaeus, C. W. Smith, W. Wanner, M.-B. Kallenrode, and G. Wibberenz, Proton and electron mean free paths: The Palmer consensus revisited, *Astrophys. J.*, 420, 294–306, 1994.
- Bieber, J., R. Burger, R. Engel, T. Gaisser, and T. Stanev, Antiprotons as probes of solar modulation, *Proc. 26th Int. Cosmic Ray Conf. Salt Lake*, 7, 17, 1999.
- Boezio, M., et al., The cosmic ray electron and positron spectra measured at 1 AU during solar minimum activity, *Astrophys. J.*, 532, 653–669, 2000.
- Cane, H. V., G. Wibberenz, I. G. Richardson, and T. T. von Rosenvinge, Cosmic ray modulation and the solar magnetic field, *Geophys. Res. Lett.*, 26(5), 565, 1999.
- Clem, J. M., D. P. Clements, J. Esposito, P. Evenson, D. Huber, J. L’Heureux, P. Meyer, and C. Constantin, Solar modulation of cosmic electrons, *Astrophys. J.*, 464, 507–515, 1996.
- Daugherty, J. K., R. C. Hartman, and P. J. Schmidt, A measurement of Cosmic Ray Positron and Negatron spectra between 50 to 800 MV, *Astrophys. J.*, 198, 493–505, 1975.
- Evenson, P., Cosmic ray electrons, *Space Sci. Rev.*, 83, 63–73, 1998.
- Evenson, P., and P. Meyer, Solar modulation of cosmic ray electrons 1978–1983, *J. Geophys. Res.*, 89, 2647–2654, 1984.

- Evenson, P., M. Garcia-Munoz, P. Meyer, K. R. Pyle, and J. A. Simpson, A quantitative test of solar modulation theory: The proton, helium and electron spectra from 1965 through 1979, *Astrophys. J.*, 275, L15, 1983.
- Evenson, P., D. Huber, E. Patterson, J. Esposito, D. Clements, and J. Clem, Cosmic electron spectra 1987–1994, *J. Geophys. Res.*, 100, 7873–7875, 1995.
- Fanselow, J. L., R. C. Hartman, R. H. Hildebrand, and P. Meyer, Charge composition and energy spectrum of primary cosmic-ray electrons, *Astrophys. J.*, 158, 771–780, 1969.
- Fassò, A., A. Ferrari, A. Ranft, P. R. Sala, G. R. Stevenson, and J. M. Zazula, A comparison of FLUKA simulations with measurements of fluence and dose in calorimeter structures, *Nucl. Instrum. Methods Phys. Res., Sect. A*, 332, 459–468, 1993.
- Fassò, A., A. Ferrari, A. Ranft, and P. R. Sala, *Proceedings of the 2nd Workshop on Simulating Accelerator Radiation Environment, SARE-2, CERN-Geneva, October 9–11 1995*, CERN Div. Rep. CERN/TIS-RP/97-05, p. 158, CERN, Geneva, 1997.
- Ferrando, P., et al., Latitude variation of  $\sim 7$  MeV and  $>300$  MeV cosmic ray electron fluxes in the heliosphere: Ulysses COSPIN/KET results and implications, *Astron. Astrophys.*, 316, 528–537, 1996.
- Fisk, L. A., Motion of the footpoint of heliospheric magnetic field lines at the Sun: Implications for recurrent energetic particle events at high heliographic latitudes, *J. Geophys. Res.*, 101, 15,547–15,553, 1996.
- Fujii, Z., and F. McDonald, Study of the properties of the step decrease in galactic and anomalous cosmic rays over solar cycle 21, *J. Geophys. Res.*, 100, 17,043–17,052, 1995.
- Fulks, G. J., Solar modulation of galactic cosmic ray electrons, protons, and alphas, *J. Geophys. Res.*, 80, 1701–1714, 1975.
- Fulks, G. J., and P. Meyer, Cosmic ray electrons in the atmosphere, *J. Geophys. Res.*, 40, 751–759, 1974.
- Garcia-Munoz, M., P. Meyer, K. R. Pyle, J. A. Simpson, and P. Evenson, The dependence of solar modulation on the sign of the cosmic ray particle charge, *J. Geophys. Res.*, 91, 2858–2866, 1986.
- Golden, R. L., S. A. Stephens, B. G. Mauget, G. D. Badhwar, R. R. Daniel, S. Horan, J. L. Lacy, and J. E. Zipse, Observation of cosmic ray positrons in the region from 5 to 50 GeV, *Astron. Astrophys.*, 188, 145–154, 1987.
- Hartman, R. C., and C. J. Pellerin, Cosmic-ray positron and negatron spectra between 20 and 800 MeV measured in 1974, *Astrophys. J.*, 204, 927–933, 1976.
- Heber, B., et al., Differences in the temporal variations of galactic cosmic ray electrons and protons: Implications from Ulysses at solar minimum, *Geophys. Res. Lett.*, 26, 2133–2136, 1999a.
- Heber, B., et al., Charge sign dependence modulation: Ulysses COSPIN/KET results, *Proc. 26th Int. Cosmic Ray Conf. Salt Lake, SH 3.2.04*, 7, 99, 1999b.
- Hovestadt, D., P. Meyer, and P. J. Schmidt, A detector system for cosmic ray electrons, *Nucl. Instrum. Meth.*, 85, 93–100, 1970.
- Howard, R., Studies of solar magnetic fields, *Sol. Phys.*, 38, 283–299, 1974.
- Jokipii, J. R., Transport and acceleration of energetic particles in winds, in *Cosmic Winds and the Heliosphere*, edited by J. R. Jokipii, C. P. Sonett, and M. Giampapa, pp. 833–855, Univ. of Ariz. Press, Tucson, 1997.
- Jokipii, J. R., and E. H. Levy, Effects of particle drifts on the solar modulation of galactic cosmic rays, *Astrophys. J.*, 213, L85, 1977.
- Jokipii, J. R., J. J. L'Heureux, and P. Meyer, Diurnal intensity variation of low-energy electrons observed near the polar cap, *J. Geophys. Res.*, 72, 4375–4382, 1967.
- Lean, J., J. Beer, and R. Bradley, Reconstruction of solar irradiance since 1610: Implications for climate change, *Geophys. Res. Lett.*, 22, 3195–3198, 1995.
- Lin, H., J. Varsik, and H. Zirin, High-resolution observations of the polar magnetic fields of the Sun, *Sol. Phys.*, 155, 243–256, 1994.
- Lockwood, M., and R. Stamper, Long-term drift of the coronal source magnetic flux and the total solar irradiance, *Geophys. Res. Lett.*, 26, 2461–2464, 1999.
- McDonald, F., Cosmic-ray modulation in the heliosphere, *Space Sci. Rev.*, 83, 33–50, 1998.
- Moraal, H., J. R. Jokipii, and R. A. Mewaldt, Heliospheric effects on cosmic-ray electrons, *Astrophys. J.*, 367, 191, 1991.
- Moskalenko, I. V., and A. W. Strong, Production and propagation of cosmic ray positrons and electrons, *Astrophys. J.*, 493, 694–707, 1998.
- Protheroe, R., On the nature of the cosmic ray positron spectrum, *Astrophys. J.*, 254, 391–397, 1982.
- Smith, E., The heliospheric current sheet and modulation of galactic cosmic rays, *J. Geophys. Res.*, 95, 18,732–18,743, 1990.
- Webb, D. F., J. M. Davis, and P. S. McIntosh, Observations of the reappearance of polar coronal holes and the reversal of the polar magnetic field, *Sol. Phys.*, 92, 109–132, 1984.

J. M. Clem, P. Evenson, and R. Pyle, Bartol Research Institute, University of Delaware, Newark, DE 19716. (clem@bartol.udel.edu; penguin@bartol.udel.edu; pyle@bartol.udel.edu)

D. Huber, Research Support Instruments, 4325 Forbes Boulevard, Suite B, Lanham, MD 20706.

C. Lopate and J. Simpson, LASR, University of Chicago, Chicago, IL 60637. (lopate@odysseus.uchicago.edu; simpson@odysseus.uchicago.edu)

(Received March 24, 2000; revised June 7, 2000; accepted June 8, 2000.)

